Evaluation of the Phonon Mean Free Path in Thin Films by using Classical Molecular Dynamics

Soon-Ho Choi and Shigeo Maruyama

Department of Mechanical Engineering, The University of Tokyo, Tokyo, Japan

Kyung-Kun Kim and Jung-Hye Lee

Division of Marine System Engineering, Korea Maritime University, Pusan, Korea

A non-equilibrium molecular dynamic (NEMD) study has been performed to evaluate the phonon mean free path (MFP) of a solid material. Solid argon with a Lennard-Jones (L-J) potential is selected as a simulation material. The thermal conductivity of a thin film plays an important role in the design of nano-electro-mechanical systems (NEMS) or micro-electro-mechanical systems (MEMS) since heat removal from these devices is a crucial factor for their intended proper operations. The values calculated by using molecular dynamics (MD) simulations are compared with the available bulk experimental data when possible. It is confirmed that there is apparently a size effect on the thermal conductivity, which indicates that the microscale system has a lower thermal conductivity than that of the bulk material in the heat transfer direction. The dependence of the thermal conductivity on the system size is the result of a reduction in the phonon mean free path (MFP) as the system size becomes microscaled, and the MD simulations can be used to predict the phonon MFP of such a system.

I. INTRODUCTION

Recently, rapid progress in and development of nanometer-sized devices have been achieved in micro-electro-mechanical systems (MEMS) and nano-electro-mechanical systems (NEMS). For example, nanoscale manufacturing technology has allowed progress from large-scale integrated circuits (LSICs) to very large-scale integrated circuits (VLSICs), and it is improving the performance of semiconductors with more compacted sizes in related industries. The reduced sizes of these devices require them to have an increased ability to dissipate the heat energy produced during their operation. Therefore, the analysis of thermal phenomena in thin films is crucial to their intended proper operations.

Another example is a superlattice, which is an artificial film that does not exist in nature. It can be made owing to the recent development of thin-film-deposition technology, which can control the thickness to a one-atom layer nowadays. Actually, the kinds of supperlattices are unlimited because they can be manufactured from arbitrary selections of any element. Their thermal conductivities and extremely high thermal resistances open the possibility of applications as new thermal insulators [1-8].

Many studies were carried out to evaluate the thermal conductivity of thin films. Most of those studies reported that the thermal conductivity of a thin film was appreciably lower than that of the bulk material and that the conventional theory based on a macroscale system, which is known as Fourier's Law, was not applicable to a microscale system [9-15]. However, there are neither experimental results nor theoretical results to predict quantitatively the variation of the thermal conductivity with the thickness of a thin film. This study was performed to clarify how the thermal conductivity varied with changes in the system size using a non-equilibrium molecular dynamic (NEMD). Solid argon was selected as a simulation material because it can be represented by the Lennard-Jones (L-J) potential of Eq.

(1), which is the simplest intermolecular potential. Moreover, there is no need to consider the contribution of free electrons to the thermal conductivity because argon is electrically a non-conductor, which means that energy transportation is caused only by the lattice vibration.

$$\varphi_{LJ}(r) = 4 \cdot \varepsilon_{AR} \left\{ \left(\frac{\sigma_{AR}}{r} \right)^{12} - \left(\frac{\sigma_{AR}}{r} \right)^{6} \right\}. \quad (1)$$

In Eq. (1), the first term on the right-hand side presents the repulsive force and the second term the attractive force; r is the intermolecular separation between two molecules, σ_{AR} the diameter of an argon molecule and ε_{AR} the depth of the potential well. Figure 1 shows the intermolecular potential energy, Eq. (1), between two argon molecules. The intermolecular force can be calculated by differentiating Eq. (1) and is given by

$$F_{LJ}(r) = -\frac{d\varphi_{LJ}(r)}{dr} = 24 \cdot \varepsilon_{AR} \left\{ 2 \cdot \left(\frac{\sigma_{AR}}{r} \right)^{12} - \left(\frac{\sigma_{AR}}{r} \right)^{6} \right\} \frac{1}{r}. \quad (2)$$

II. SIMULATION METHOD

Although solid argon has limited applicability in real situations, it was selected as the simulation material because the results can be used as a benchmark with which further study of other material systems can be compared. The simulation system was arranged with the fcc<111> as shown in Fig. 2. An adiabatic wall, which is composed of 3 layers, is placed at the bottom and the top for the purpose of isolating the system from the environment. Another 3 layers are placed on the adiabatic wall for temperature control. The bottom is controlled at a high temperature and the top at a low temperature so that heat flows up (z direction). The x-y

plane perpendicular to the direction of heat flow is set as a periodic boundary condition (PBC), which mimics well the configuration of an actual thin film [17-19].

The velocity scaling method is used for temperature control and the equation of motion is integrated by using the Velocity Verlet method [16-22]. The intermolecular distance is determined so as to maintain the system in a free-standing state, which means a system to be under the zero stress state internally during a simulation [23-24]. The details that describe the intermolecular distance under a freestanding state will be given in the section III-1.

Eighteen argon molecules are arranged on x and y directions, respectively, per layer, and the system has a total of 30 layers in the z direction. The temperature gradient is measured in eighteen layers excluding the temperature control layers (TCLs) and the adiabatic wall at each side. The time interval for an iteration of the equation of motion is selected as $\Delta t = 1.0 \times 10^{-15}$ s (= 1 fs) and the properties of argon are $\sigma_{AR} = 3.4$ Å, $m_{AR} = 6.634 \times 10^{-26}$ kg, and $\varepsilon_{AR} = 1.67 \times 10^{-21}$ J [16-19].

In the MD simulation the intermolecular force calculation is the most time-consuming procedure, so almost all MD codes use the concept of a cut-off length [20-22]. As shown in Fig. 1, the intermolecular potential is nearly zero if two molecules are separate by more than 2.5 σ_{AR}. Therefore, it is useless to consider the effects from molecules far from that length when calculating the intermolecular force. Generally the recommended cut-off length is 2.5 σ_{AR} [21-24]. However we determined it to be 3.5 σ_{AR} from our experience with other simulations [16-19]. Our MD simulations consist of a series, in which the first simulation puts the system be in an initial equilibrium state at a given temperature and then, it is relaxed during some period for the assurance of a fully equilibrated state. In the third simulation, controlling each TCLs individually develops a temperature gradient using the velocity scaling method described as [20-22]

$$v_{new}\big|_i = v_{old}\big|_i \sqrt{\frac{T_{des}}{T_i}} \,. \tag{3}$$

In Eq. (3), v_{new} and v_{old} are the velocities of molecule i after and before the velocity scaling, respectively. T_{des} is the desired temperature to be maintained and T_i is the instantaneous temperature of molecule i.

The simulations after the third one are for developing a temperature gradient and are performed eleven times, each involving 200,000 iterations (200 ps), however, the first is excluded in the evaluation of the thermal conductivity because a transient period is necessary for a temperature gradient to develop in a system. Therefore, the thermal conductivity is the averaged value over the last ten simulations. The initial equilibrium temperatures are set to 10 K and 40 K, that is, two cases were investigated. In both cases, after achieving an equilibrium state, the temperature difference of 4 to 6 K was created in the system by controlling the TCLs. The average temperature of a system in each case was confirmed as 10 K and 40 K, respectively, during all simulations although each TCL is set at a different temperature.

III. RESULTS AND DISCUSSION

1. INTERMOLECULAR DISTANCE UNDER A FREE-STANDING STATE

The thermal conductivity of a non-conductor such as argon might be affected by the internal stress because the transport of the lattice vibration energy will be facilitated as the intermolecular separation is decreased. When an MD simulation is performed on a microscale system, any trivial change in the intermolecular distance results in great internal stress so the pressure effect on the thermal conductivity has to be investigated. If that is not done, the

calculated thermal conductivity will contain an additional effect due to the internal stress.

For the determination of the intermolecular length under a free-standing state, another simulation is carried out on the system with 3-dimensional periodic boundary conditions (PBCs) shown as Fig. 3, which is different from Fig. 2 because it has no adiabatic wall and is a smaller sized system. Each snapshot is an equilibrium state of the system, but at a different temperature. The figure shows that the magnitude of a molecule's motion becomes more severe as the temperature of the system is increased.

Figure 4 (a) shows the internal pressure calculated by using the virial theorm of Eq. (4), which is measured at equilibrium temperatures of 10 K, 40 K and 60 K [17-24].

$$p = \frac{2N}{3V}\left\langle E_k \right\rangle + \frac{1}{3V}\sum_{i=1}^{N-1}\sum_{j=i+1}^{N} F_{ij} \cdot r_{ij} \tag{4}$$

In Eq. (4), V is the volume of the system, N the total number of molecules in the system, r_{ij} the intermolecular distance between molecules i and j, F_{ij} the intermolecular force, and $\langle E_k \rangle$ the average kinetic energy of the system during a simulation. The pressures are calculated by changing the intermolecular length of the fcc<111> arrangement. Fig. 4 (a) is the intermolecular length for which the system is in the zero stress state at respective equilibrium temperatures and is determined from a linear fitting of the calculated pressures. The internal stress is found to be more sensitive to the intermolecular length when the temperature of a system is low.

Figure 4 (b) shows the variation of the intermolecular length with the dimensionless system temperature for a free-standing state; the results of Brougton and Gilmer [24] and the experimental results [25] are also shown for comparison. The results of Brougton and Gilmer seem to fit with the experimental results in the low temperature region better than the results of this study; however, the overall shape of the curve obtained in this study is much more

closer to the shape of the experimental curve. The intermolecular lengths at 10 K and 40 K, at which all simulations are carried out to clarify the size effect on a thermal conductivity, are r_o=1.0969 σ_{AR} and r_o=1.1115 σ_{AR}, respectively, for a free-standing state. The fitting curve based on this result can be presented as

$$r_0(T) = C_0 + C_1 T + C_2 T^2 \tag{5}$$

where C_0 = 1.09294, C_1 = 3.73333 x 10^{-4}, and C_1 = 2.26667 x 10^{-6}.

2. CALCULATION OF THE THERMAL CONDUCTIVITY

There are two methods for determining the thermal conductivity. One calculates the thermal conductivity measuring the temperature gradient that develops in a system under a given heat flux while the other does it by the measuring of the heat flux that passes through a system under a given temperature gradient. In real experiments, the thermal conductivity is generally evaluated by using the former. NEMD intrinsically uses the former method because a heat flux is given to a system so that both TCLs can be maintained to any desired temperature. The heat flux is determined from the energy applied to the hot temperature control layers (HTCLs) or taken from the cold temperature control layers (CTCLs) in order to maintain them to any set temperature. Therefore, the heat flux can be calculated by

$$q_{in} = \frac{1}{2}\sum_{j=1}^{n_{TC}}\sum_{i=1}^{N_H} m_{AR}\left(v_{new}\big|_i^2 - v_{old}\big|_i^2\right), \tag{6}$$

$$q_{out} = \frac{1}{2}\sum_{j=1}^{n_{TC}}\sum_{i=1}^{N_L} m_{AR}\left(v_{old}\big|_i^2 - v_{new}\big|_i^2\right), \tag{7}$$

$$\dot{q}_{in} = \frac{q_{in}}{n \cdot \Delta t}, \tag{8}$$

$$\dot{q}_{out} = \frac{q_{out}}{n \cdot \Delta t}. \tag{9}$$

In the above equations, n is total number of iteration in a simulation, and n_{TC} is the number of temperature controls performed in that simulation. N_L and N_H are the numbers of molecules included in the HTCLs and the CTCLs respectively. Figure 5 gives examples of a heat flux and a temperature gradient obtained from a simulation. The upper line of Fig. 5 (a) is the accumulated energy applied to the HTCLs, and the lower line is that taken from the CTCLs. From this figure, the system is considered to be fully in a non-equilibrium steady state because almost the same heat fluxes exist at the two TCLs. The slopes of these accumulated energies are calculated per unit area, and correspond to a heat flux. The temperature gradient corresponding to the state of Fig. 5 (a), which is shown in Fig. 5 (b), is the average temperature of the molecules per layer over a simulation, and it is a linear fit excluding both TCLs. However, the heat flux of the CTCLs is used for the calculation of the thermal conductivity because it is an actual heat current out of the system.

The size effect on the thermal conductivity is investigated by performing simulations for various system lengths in the heat flow direction. The shortest system is six layers except for both TCLs, and the system is increased by 6 layers in length up to the longest one of 54 layers. Figure 6 shows the dependence of the thermal conductivity on the length. In Fig. 6, the experimental data of Dobbs and Jones for a bulk state are also shown for comparison [25].

The simulations are carried out in the way described in Section II so that the calculated thermal conductivities are average values over ten simulations for each case.

Each error bar shown in Fig. 6 (a) is a standard deviation that shows the distribution of all data for each case, that is, $3 \cdot \sigma_{STD}$. This figure indicates that the thermal conductivity increases as the length of a system becomes longer and eventually becames equal to that of the bulk state if the system is longer than a specified length. It is natural to deduce from the linear fitting lines of Fig. 6 (a) that a hot system should be lengthy in order to have a thermal conductivity equal to that of a bulk. However, it must be noted that the fitting lines do not imply the above description at all. The actual situation is rather to the contrary, which means that a cold system requires a longer length to have a thermal conductivity equal to that of a bulk state, which can be explained based on the concept of the phonon mean free path (MFP). Figure 6 (b) shows the same results as Fig. 6 (a) except that the scales of the axes are reversed for application of the phonon concept and the figure excludes data shorter than 100 Å in length. The details will be described in the next section. Consequently, the fitting lines in Fig. 6 (a) are only guides for the eye.

3. PHONON MEAN FREE PATH

The thermal conductivity of a solid material can be interpreted by using the phonon mean free path (MFP), which originates from the kinetic theory of gases [26] and is given by

$$\lambda = \frac{1}{3} c_V v_P l_P \,. \tag{10}$$

In the case of solids, c_V, v_P, and l_P are the specific heat capacity of a phonon, the phonon velocity inherent in a material, which is often explained as an acoustic velocity, and a phonon

MFP while in the case of gases, they represent the specific heat capacity of gases under a constant volume, the average molecular velocity, and the MFP between the intermolecular collisions, respectively [27]. However, it is impossible to expect a quantitatively accurate thermal conductivity from Eq. (10) based on some oversimplified assumptions. Hence, Eq. (10) should be considered as providing the qualitative behavior of a thermal conductivity from which the thermal conductivity is found to be proportional to the phonon MFP. Also, the phonon MFP is well known to become shorter as the system is hotter because the phonon population is increased, which causes the collision frequency among phonons to be high. Increased phonon collisions prevent the phonons with high energy in the hot region from moving to the cold region and vice versa. This means that the energy transport is low; consequently, the thermal conductivity is low [19]. Therefore, it can be inferred that phonon scattering governs the thermal conductivity.

Phonon scattering in a solid consists of four processes, which are collisions among (a) phonons, (b) phonons and any defects that exists in the system, (c) phonons and free electrons, and (d) phonons and boundaries of the system. However two scatterings, (b) and (c), can be completely ignored because there are no free electrons in argon and structural defects do not exist in perfect crystals like the ones of this study. The phonon MFP can be written as follows if only (a) and (d) are considered [18, 19] :

$$\frac{1}{l_P} = \frac{1}{l_{BULK}} + \frac{1}{l_{SYS}}. \tag{11}$$

In Eq. (11), l_{BULK} is the phonon MFP in the bulk state and l_{SYS} the length of the system. The meaning of Eq. (11) is that l_P should be equal to l_{BULK} if the system is in the bulk state, so l_{SYS} is infinite. Therefore, l_{SYS} does not contribute to the phonon MFP in the bulk state; however, it dominates the phonon MFP as the system decreases in size. Under the condition that the

thickness of the thin film is shorter than the phonon MFP in the bulk state, $1/l_P$ will be a linear relation in $1/l_{SYS}$ because $1/l_{BULK}$ can be treated as a constant. From this interpretation and Eq. (10), one can easily understand that the inverse of the thermal conductivity is linearly proportional to the inverse of the system size in the direction of heat flux :

$$\frac{1}{\lambda} = \frac{3}{c_V v_P} \frac{1}{l_P}. \tag{12}$$

Figure 6 (b) emphasizes of the linear relation between $1/\lambda$ and $1/l_{SYS}$. In this figure, the difference between MD results and the experiment is about 10 % in both cases. This difference is sufficiently acceptable for engineering purposes and will be reduced if additional data for a longer system are included. The form of the fitting line shown in Fig. 6 (b) and Eq. (12) should be noted since they eventually have the same forms :

$$\frac{1}{\lambda} = A\left(\frac{1}{l_{SYS}} + \frac{1}{l_{BULK}}\right) \qquad \left[A = \frac{3}{c_V v_P}\right]. \tag{13}$$

$$\frac{1}{\lambda} = \frac{A}{l_{SYS}} + B \qquad \left[l_{BULK} = \frac{A}{B}\right]. \tag{14}$$

From Fig. 6 (b) and Eq. (14), it is clear that the MD simulations provide information on the variation of the thermal conductivity of a thin film with changes in its thickness. Aside from complete agreement between the thermal conductivities from MD simulations and those from experiments, the thermal conductivities of thin films can be determined from the slope of the fitting line and the intersection with the vertical axis. If we accept the intersections with the vertical axis in Fig. 6 (b) as the thermal conductivity of solid argon in the bulk state, $\lambda_{\mathrm{BULK@10}}$

$_{K}$ is 3.333 W/(m·K) and $\lambda_{BULK@40\,K}$ is 0.604 W/(m·K). The phonon MFP in the bulk state is also evaluated as $l_{P@10\,K\,in\,BULK}$=122 Å and $l_{P@40\,K\,in\,BULK}$=34 Å by Eq. (14). These values are reasonable since many more phonons exist in a hot system than in a cold system, so the phonon MFP is shorter in a hot system due to their frequent collisions, as described previously.

Figure 7 is the thermal conductivities at 10 K and 40 K calculated by using Eq. (14) and shows that the size effect on the thermal conductivity can be evaluated by using MD simulations. This obviously indicates that a cold system must be lengthy compared with a hot one in order to have the same thermal conductivity as the bulk state.

Figure 7 provides the opposite situation compared with Fig. 6 (a) and implies that a hot system must be longer than a cold system in order to have the bulk thermal conductivity. This discrepancy results from l_P in Eq. (10) not including the size effect; thus, the fitting lines in Fig. 6 (a) are presented for the purpose of providing guides for the eye.

IV. CONCLUSION

This study shows that the phonon mean free path (MFP) of a thin film can be calculated using MD simulations, which provide reasonable results with no contradiction with considerations based on phonon theory. However, we emphasize that the results of this study are only applicable for an electrical insulator because free electrons in a conductor, such as a metal play a major role in heat transfer. Nevertheless, we are certain that the method of this study provides a simple tool to evaluate the thermal conductivity of a microscale thin film, such as the substrate of a semiconductor.

[1] T. Shinjo and T. Takada, Metallic Superlattices-Artificially Structured Materials

(Elsevier, Amsterdam, 1987).

[2] B. C. Daly and H. J. Maris, Physica B **316-317**, 247 (2002).

[3] G. Chen and M. Neagu, Appl. Phys. Lett. **71**, 2761 (1997).

[4] W. S. Capinski, M. Cardona, D. S. Katzer, H. J. Maris, K. Ploog and T. Ruf, Physica B **263-264**, 530 (1999).

[5] P. Hyldgaard and G. D. Mahan, Phys. Rev. B **56**, 10754 (1997).

[6] T. Yao, Appl. Phys. Lett. **51**, 1798 (1987).

[7] X. Y. Yu and G. Chen, Appl. Phys. Lett. **67**, 3554 (1995).

[8] S. H. Choi, S. Maruyama, K. K. Kim and J. H. Lee, Accepted, J. Korean Phys. Soc. (2003).

[9] D. G. Cahill, W. K. Ford, K. E. Goodson, G. D. Mahan, A. Majumda, H. J. Maris, R. Merlin and S. R. Phillpot, J. Appl. Phys. **93**, 793 (2003).

[10] E. T. Swartz and R. O. Pohl, Rev. Mod. Phys. **61**, 605 (1989).

[11] G. Chen, J. Nanoparticle Res. **2**, 199 (2000).

[12] G. Chen, ASME J. Heat Transfer **119**, 220 (1997).

[13] M. I. Flik, B. I. Choi and K. E. Goodson, ASME J. Heat Transfer **114**, 666 (1992).

[14] P. K. Shelling, S. R. Phillpot and P. Keblinski, Phys. Rev. B **65**, 144306 (2002).

[15] F. C. Chou J. R. Lukes, X. G. Liang, K. Takahashi and C. L. Tien, Ann. Rev. Heat Transfer **10**, 141 (1999).

[16] S. H. Choi and S. Maruyama, Proc. of 37th National Heat Transfer Symp. of Japan (Kobe, 2000).

[17] S. H. Choi and S. Maruyama, Proc. of 39th National Heat Transfer Symp. of Japan (Sapporo, 2002).

[18] S. H. Choi and S. Maruyama, Proc. of 40th National Heat Transfer Symp. of Japan (Hiroshima, 2003).

[19] S. H. Choi, Ph. D. dissertation (The University of Tokyo, 2003).

[20] D. Frenkel and B. Smit, Understanding Molecular Dynamics (Academic Press, San Diego, 1996).

[21] J. M. Haile, Molecular Dynamics Simulation : Elementary Methods (John Wiley & Sons, New York, 1997).

[22] R. J. Sadus, Molecular Simulation of Fluids (Elsevier, Amsterdam, 1999).

[23] H. Kaburaki J. Li and S. Yip, Proc. of Mat. Res. Soc. Symp. **538**, 503 (1999).

[24] J. Q. Broughton and G. H. Gilmer, J. Chem. Phys. **70**, 5095 (1983).

[25] E. R. Dobbs and G. O. Jones, Rep. Prog. Phys. **20**, 516 (1957).

[26] F. Reif, Fundamentals of Statistical and Thermal Physics (McGraw-Hill, London, 1985)

[27] Charles Kittel, Introduction to Solid State Physics (Wiley, New York, 1996).

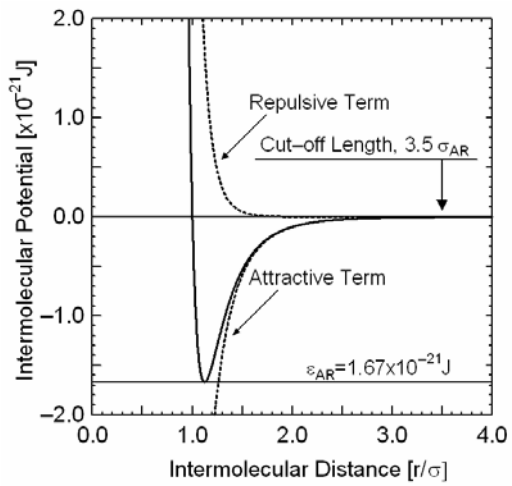

FIG. 1. Lennard-Jones (L-J) potential with an intermolecular length.

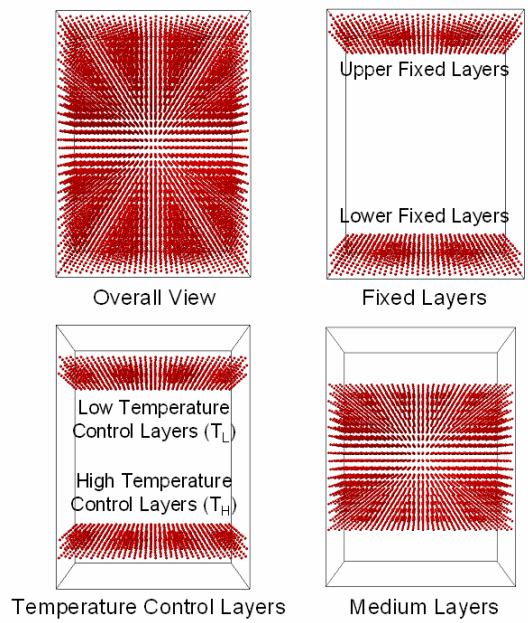

FIG. 2. The simulation system with an adiabatic wall. The size of a system is the example of 18 x 18 molecules in the x-y plane and 30 layers in the z direction. The heat energy flows up (+z direction).

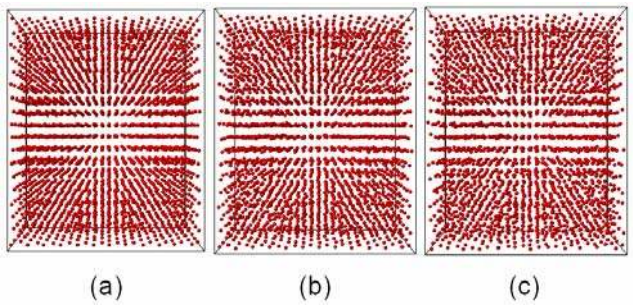

FIG. 3. Simulation system for calculating the system pressure : (a) 10 K, (b) 40 K, and (c) 60 K. The size of the system is 12 x 12 x 18, the boundary conditions of which are 3-dimensional periodic boundary conditions.

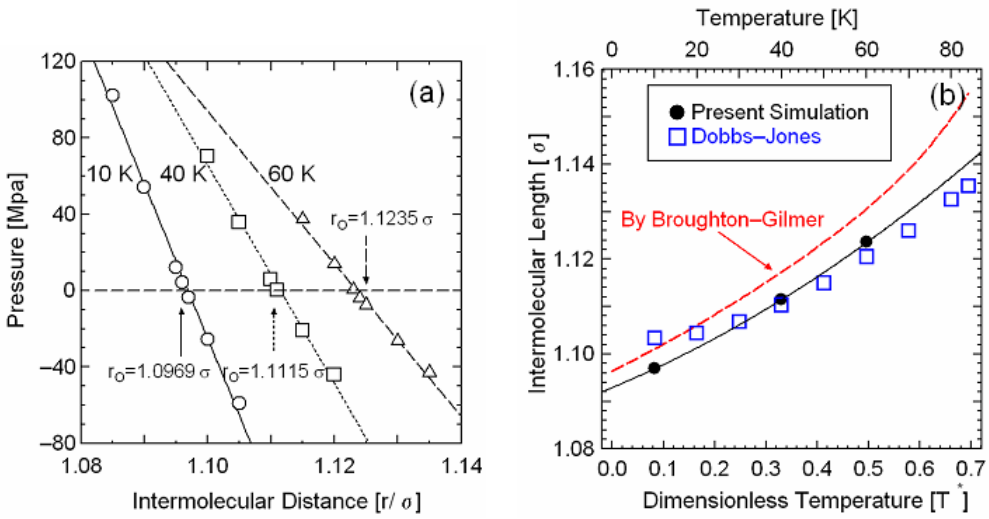

Fig. 4. (a) Pressure as a function of the intermolecular length and (b) intermolecular length as a function of the dimensionless temperature for a free-standing state.

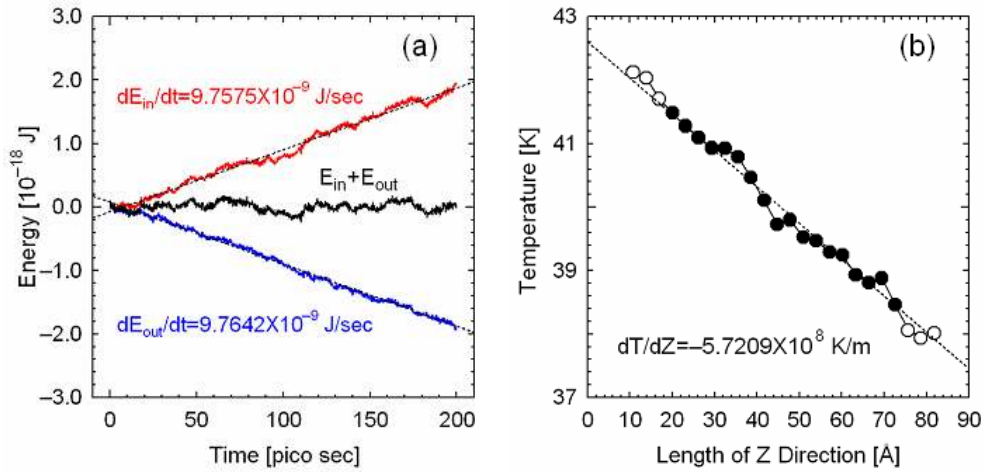

Fig. 5. (a) Heat flux and (b) temperature profile obtained by using the velocity scaling method at T_{ave} = 40 K for a system size of 68 Å x 59 Å x 55 Å.

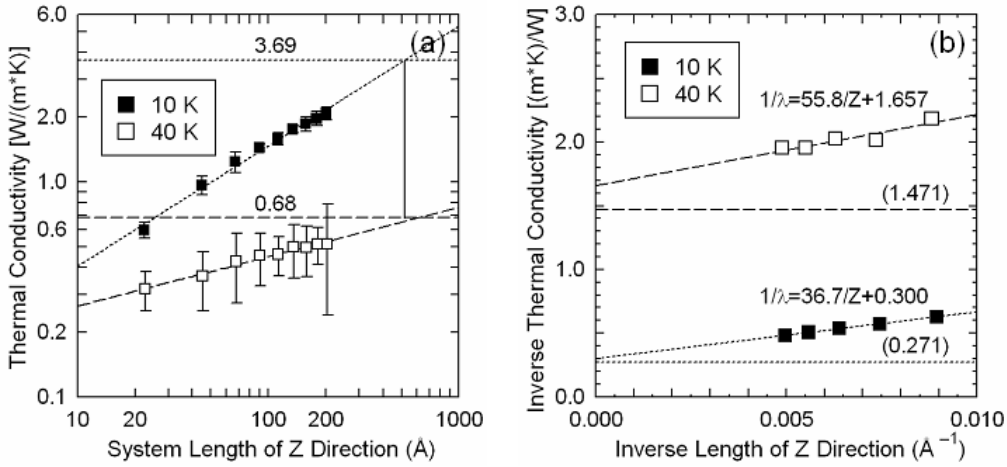

Fig. 6. Dependences of the thermal conductivities on the system size : (a) log-log scale and (b) inverse scale.

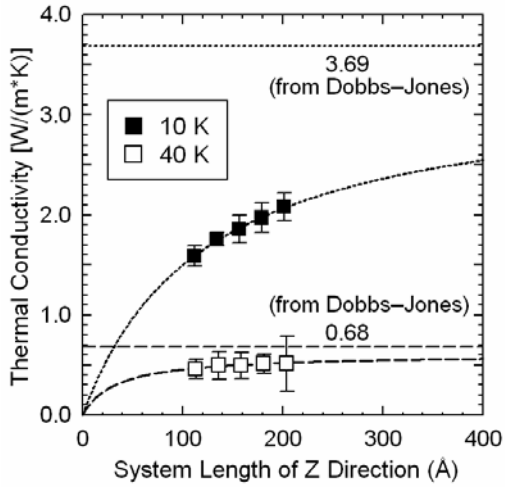

FIG. 7. Variation of the thermal conductivity of solid argon films with the thickness.